SUPPORTING INFORMATION

Molecular Mechanisms of Toxicity of Silver Nanoparticles in Zebrafish Embryos

Ronny van Aerle[1], Anke Lange[1], Alex Moorhouse[1], Konrad Paszkiewicz[1], Katie Ball[1], Blair D. Johnston[1,2], Eliane de-Bastos[1], Timothy Booth[3], Charles R. Tyler[1§], Eduarda M. Santos[1§]*

[1] Biosciences, College of Life and Environmental Sciences, Geoffrey Pope Building, University of Exeter, Stocker Road, Exeter, EX4 4QD, UK.

[2] Comprehensive Pneumology Center (CPC), Institute of Lung Biology and Disease (iLBD), Helmholtz Zentrum München, Deutsches Forschungszentrum für Gesundheit und Umwelt (GmbH), Ingolstädter Landstr. 1, 85764 Neuherberg, Germany

[3] NBAF-W, Centre for Ecology & Hydrology (CEH) Wallingford, Benson Lane, Wallingford, OX10 8BB, UK.

*Corresponding author: Tel: +44 1392 725845; Fax: 00 44 1392 263700; E-mail: r.van-aerle@exeter.ac.uk.

This Supporting Information contains:

There are also a number of separate Supplemental Files:

File S1 – Perl script used to remove all bases after the last occurrence of CATG (*Nla*III restriction site, used for the preparation of the HT-SuperSAGE libraries) in each of the sequences in a FASTA file (compressed TXT file)

File S2 – Perl scripts used for totalling counts of unitags for each gene and discarding unitags that mapped to multiple genes (compressed TXT file). The four scripts were designed to be run in sequence to produce a tag frequency table. At any point in the pipeline, intermediate results may be saved out in JSON format for inspection.

File S3 - Overview of the expression of all genes for all treatments (XLS). Data given for the complete dataset and for differentially expressed genes for each treatment include Ensembl gene ID, total count numbers, normalized count numbers (counts per million), fold change, P values, gene name and gene description.

File S4 – Comparison of HT-SuperSAGE and Affymetrix microarray data (XLS). Details are provided in the Excel spreadsheet.

File S5 – Gene Ontology and KEGG pathway over-representation in differentially expressed gene lists following exposure of zebrafish embryos to the various silver treatments for 24 and 48h (XLS). Over-representation analysis was conducted for gene lists differentially expressed between each treatment and its control (adjusted P values < 0.05) using the list of all expressed genes as a background, within DAVID.

File S6 – Effects of the various silver treatments on the transcription of genes belonging to the mitochondrial dysfunction and oxidative phosphorylation pathways (PDF). Shades of green and red represent progressive down-regulation and up-regulation of target genes, respectively. (a-f) Effects of exposure to the various silver treatments on the mitochondrial dysfunction pathway. (g-l) Effects of exposure to the various silver treatments on the oxidative phosphorylation pathway. Pathways were generated

through the use of Ingenuity Pathways Analysis (Ingenuity® Systems, www.ingenuity.com).

SUPPLEMENTAL EXPERIMENTAL SECTION

Materials and characterization of the silver particles

Silver particles (designated as AgNP, and Ag Bulk) were purchased from Nanostructured and Amorphous Materials Inc., Houston, USA. Based on the manufacturers specifications, AgNP were spherical particles of average size 10 nm, with a specific surface area of 9–11 m^2/g, bulk density of 2.05 g/cm^3 and a true density of 10.5 g/cm^3, and had a purity of 99.9%, based on trace metal analysis. Bulk silver particles had an average particle size of 0.6–1.6 μm and purity of 99.95%. Silver with 2% HNO_3 was obtained from PerkinElmer Life and Analytical Sciences, Connecticut, USA. The characterization of the exposure particles has been described previously [1] in which particle size, shape and charge were established using (high resolution) transmission electron microscopy (HRTEM), atomic force microscopy (AFM), X-ray electron dispersive spectroscopy (X-EDS), X-ray diffraction (XRD), dynamic light scattering (DLS) and the Braun Emmett Teller (BET) method of specific surface area analysis. In summary, the AgNP had the most negative average zeta potential value (-12.5 mV) and formed aggregates of 589 ± 101nm (measured by Dynamic Light Scattering [DLS]). These particles had a polydispersity index of 0.54, indicating relatively uniform aggregate sizes. The average zeta potential for Ag Bulk was -2.8 mV, and these particles formed aggregates of 938 ± 230nm (DLS) and had a polydispersity index of 0.69. Electron microscopy images confirmed the potential of the particles to aggregate and further details of the characterization of these particles are given in [1].

Assessment of the dissolution of silver particles in exposure medium

AgNP and Ag Bulk were dissolved in ultrapure water as described in the main manuscript. Four beakers were set up with 800 mL of artificial water, prepared according to the ISO 7346-3:1996 guideline and placed on a magnetic stirrer. Four sealed dialysis membranes (Dialysis membrane Spectra/Por 7, Fisher), filled with10 mL of artificial water were added to each beaker. At the start of the experiment, an appropriate volume of AgNP and Ag Bulk stock solution was added to each beaker to obtain a final concentration of 5 µg silver material/L (2 replicate beakers for each treatment) and the solutions were stirred continuously for 24h, at a constant temperature of 28^{o}C. The solution contained within a dialysis membrane from each treatment replicate was sampled at 3, 6, 12 and 24h and acidified with 2% of nitric acid for determination of the concentration of Ag^{+} inside the membrane, corresponding to the dissolved Ag^{+} originating from the Ag particles. Ag content in the water samples was measured using a Thermo Scientific, X Series 2 ICP-MS instrument at the Analytical Research Facility (ARF), University of Plymouth, UK.

Embryo exposures for determination of toxicological effects in zebrafish embryos

Zebrafish embryos were exposed to a range of concentrations of Ag^{+} (0.0122 to 100 µg/L) AgNP (3.9 to 8000 µg/L) and Ag Bulk (3.9 to 8000 µg/L) in order to determine the mortality curves for each form of silver. Exposure chambers (600 mL) received 400 mL of ISO water containing the appropriate concentration of Ag^{+}, AgNP, or Ag Bulk. Twenty fertilized embryos were deployed into each treatment chamber and including control chambers which received water alone. Exposure chambers which incubated in a water bath at 28 ± 1°C with a 12h light:dark photoperiod, ensuring consistency in the exposures for all treatments. Exposures were initiated at 4hpf, and the water was changed completely 24h after the start of

the exposure. Embryo mortalities were determined at 24h and 48h after the start of the chemical exposure by visual inspection using light microscopy (Kyowa Optical SDZ PL, Kyowa Optical, Japan) and any dead embryos were removed from the exposure chambers. The experiment was terminated 48h after the start of the chemical exposures by humanely sacrificing the remaining embryos.

Embryo exposures for investigations into the effects of Ag^+ on oxygen consumption

Zebrafish embryos were exposed to a range of concentrations of Ag^+ and including those expected to be present in the water as a consequence of dissolution following exposure to AgNP, Ag Bulk and Ag^+ (0, 0.031, 0.062, 0.125, 0.250, 0.500, 1 and 5 μg Ag^+/L). Exposure chambers received 500 mL of ISO water containing the appropriate concentration of Ag^+. Groups of 5 fertilized embryos were deployed into individual glass vials, filled with exposure water and capped under water to ensure complete displacement of any air in the vials. For each treatment, 6 vials were set up, and incubated within the exposure chambers, placed in a water bath at 25.5^{o}C, to ensure consistency in exposure temperatures for all treatments, and a vial without embryos was also included as a control for the oxygen measurements. Exposures were initiated at 4hpf, and exposure water was changed completely after 24h. Concentration of oxygen was determined in the chambers and individual vials at 24 and 48h of exposure using a Strathkelvin Instruments Oxygen Meter, model 781. In this way, oxygen consumption could be determined for individual embryos, using the measurements of volume of individual vials, incubation time and difference in oxygen partial pressure (PO_2) between the exposure water without embryos and the exposure vials. Water PO_2 was converted to oxygen content using the equation (0.0000017361*(T^3)) + (0.0004068*(T^2)) - (0.0515611*(T)) + 2.6779143, derived from tabulated values for the oxygen solubility coefficient in water of

zero salinity, in which T was the temperature of each chamber [2]. Oxygen consumption (MO_2) was then calculated using the Fick principle, according to the equation MO_2 = (water volume x ΔO_2) / (number of embryos x time period). The experiment was terminated following 48 h of exposure.

HT-SuperSAGE library construction

Illumina compatible adapters used in this experiment were kindly provided by Dr Matsumura (Iwate Biotechnology Research Center, Kitakami, Japan). Double-stranded cDNA was synthesized from 5–10 μg of total RNA, primed with a poly-T biotinylated adapter containing the *Nla*III recognition site and using the SuperScript II double-stranded cDNA synthesis kit (Invitrogen). Purified cDNA was digested with the anchoring enzyme *Nla*III, and the resulting fragments were bound to beads coated with streptavidin (Dynabeads streptavidin M-270), while non-biotinylated cDNA fragments were removed. A double stranded adaptor containing the EcoP151 recognition site and 3' overhang complementary to the *Nla*III restriction site was ligated to the cDNA fragments, bound to beads and digested with EcoP151. Following digestion, released fragments were ligated to a second double stranded adapter complementary to the EcoP151 overhang and containing motifs for flowcell binding, priming the sequencing reaction and a 4 nucleotide barcode index for sample identification. Tagged fragments were amplified via PCR in 8-15 reactions per library. PCR products were pooled, concentrated using a MinElute reaction purification kit (Qiagen) and analysed on an 8% non-denaturing polyacrylamide gel. Visualization of amplicons stained with SYBR green (Invitrogen) was followed by excision and purification of a band corresponding to 123-125bp. The purified PCR product for each sample was analyzed using an Agilent Bioanalyser 2100 for accurate sizing and quantification. Equimolar concentrations

of the PCR products for each sample were pooled in groups of 3 or 4, and libraries were sequenced using an Illumina Genome Analyzer (GA) II platform.

All proprietary products were used according to manufacturer's instructions. Library preparation reaction parameters were used as described elsewhere [3].

SUPPLEMENTAL RESULTS AND DISCUSSION

Assessment of the dissolution of silver particles in exposure medium

The dissolution rates for AgNP and Ag Bulk were variable and ranged from below the detection limit of the method (0.001 μg/L) to 0.7% and 0.6% for AgNP and Ag Bulk, respectively. There was no clear association of the dissolution rates with time, suggesting that most of the dissolution may have occurred during the initial suspension of the particles in water, which involved a period of sonication. The average dissolution rate was 0.27 ± 0.15% and 0.27 ± 0.07% for AgNP and Ag Bulk, respectively.

Toxicological effects of exposure to Ag^+, AgNP and Ag Bulk in zebrafish embryos

Exposure to Ag^+, AgNP and Ag Bulk caused mortalities to zebrafish embryos in a dose response manner (Figure S1). The LC50 concentrations were 19.2, 1912.8 and 2043.4 μg/L of Ag^+, AgNP and Ag Bulk, respectively. Based on this data, the concentrations selected for the molecular analysis of the mechanisms of toxicity of the three forms of silver were far below those causing overt toxicity in our experimental conditions.

HT-SuperSAGE data analysis

The number of sequences obtained for each library ranged from 1.2 million (48 hpf AgNP) to 2.2 million (24 hpf AgNP) and the abundance distributions of these sequence tags were generally consistent between all libraries (Table S1). Importantly, despite some variation in the number of tags sequenced per treatment group, the numbers of tags corresponding to relatively abundant classes were highly consistent across treatments, and the variable numbers of tags were found to fall within the group of tags which were sequenced only once per sample. In total, 13,680,994 sequences were taken further for analysis and these were represented by 606,259 unique sequence tags (unitags). A total of 205,033 unitags were sequenced more than once across all treatments (with a total of 13,279,768 counts). Between 29 and 40% of the unitags (401,226) were sequenced only once across all treatments (referred to in this paper as singletons), but these accounted for only between 2-3% of the total number of sequences obtained (Table S1; Figure 1). This is consistent with other studies that employed the SuperSAGE methodology, although in these studies singletons were referred to as tags that were sequenced only once per sample as opposed to once across all treatments [4-7]. It cannot be excluded that some singletons may represent low-abundance transcripts or be the result of PCR/sequencing errors. However, singletons were included in the downstream analyses to avoid losing information from low-abundance transcripts.

In total 99,683 unitags aligned to zebrafish genes, with 77,821 of these mapping to unique genes only (7,690,269 counts in total) and representing 14,793 genes (Figure 1). This is consistent with previous studies that reported a similar number of expressed genes in embryos at similar stages of development using zebrafish Affymetrix microarrays (ArrayExpress database [http://www.ebi.ac.uk/arrayexpress/]; Experiment ID: E-TABM-33) or RNAseq [8]. About 20 percent of the unitags (21,872) and with a total of 221,592 counts

(3% of the total unitag counts), also mapped to antisense gene sequences, which has been observed previously in other tag-based gene expression studies [9-11]. Approximately 80% of the genes were represented by more than one unitag (see Figure S2), consistent with other studies that are based on SAGE methods, which is likely the result of incomplete *Nla*III digestion during the library preparations, alternative polyadenylation and/or alternative splicing sites [12-14].

Comparison with previous microarray study

We compared our gene expression data for controls (non-exposed) with previous (unpublished) data for zebrafish embryos at 24 and 48h of development obtained using zebrafish Affymetrix microarrays (downloaded from the ArrayExpress database; Experiment ID E-TABM-33). A comparison of the ratios of expression values of all genes for which data were available for both platforms and for both time points (48 hpf /24 hpf) identified a strong correlation between the datasets ($r = 0.714$; $P < 0.0001$; $n = 4951$) . In addition, we identified a group of genes (48 in total) that were expressed at 24h but not at 48h both in our experiments and the microarray dataset (see File S4). Many of these genes are likely to be maternally expressed genes and not transcribed during embryogenesis. As such, these genes were expected not to be regulated by the chemical exposures and indeed, we confirmed that none of these putative maternally expressed genes were differentially expressed for any treatment or time point. Conversely, a number of genes (77 in total) were only found to be expressed at 48hpf and these were predominantly involved with eye, brain and muscle development (organs known to develop during later stages of embryogenesis in zebrafish; [15]; File S4). Together, these findings support that our measurements and data analysis are highly robust.

SUPPLEMENTAL FIGURES AND TABLES

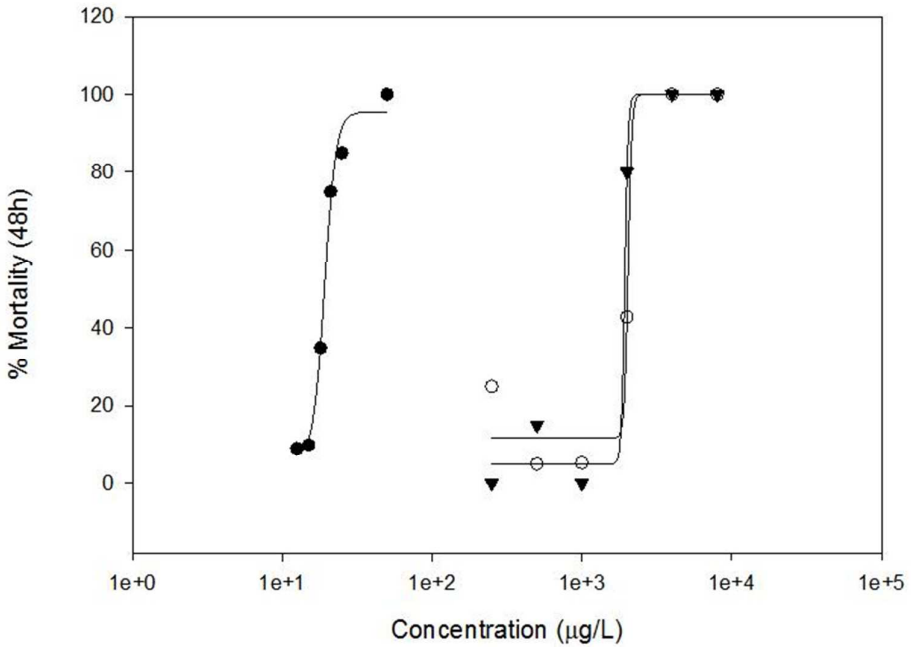

Figure S1 – Mortality curves for zebrafish embryos exposed to Ag^{+}, AgNP and Ag Bulk for 48h (between 4 and 52h post fertilization). Closed circles, closed triangles and open circles represent mortality data following exposure to Ag^{+}, AgNP and Ag Bulk, respectively.

Table S1 – Properties of the HT-SuperSAGE libraries from control and silver-treated zebrafish embryos.

For each library, the sequence tag abundance, the number of unique sequence tags (unitags) and the total number of sequence tags are given.

	24h post-fertilisation				48h post-fertilisation			
	Control	Silver NP	Silver bulk	Silver ions	Control	Silver NP	Silver bulk	Silver ions
Copies million^{-1}	**Sequence abundance**							
>10,000	6	9	12	13	10	12	11	14
1,000-10,000	77	82	85	107	95	103	92	99
100-1,000	509	648	609	585	617	700	623	684
10-100	4,431	5,527	4,834	3,940	5,343	5,820	5,165	5,593
1-10	15,408	17,493	16,058	13,631	16,515	17,170	15,509	15,368
≤1	126,117	157,429	95,317	63,417	137,620	87,100	132,155	135,446
Total	**146,548**	**181,188**	**116,915**	**81,693**	**160,200**	**110,905**	**153,555**	**157,204**
	Number of unitags							
Non-singletons	88,939	109,620	75,346	58,044	96,539	76,559	100,346	101,589
Singletons	57,609	71,568	41,569	23,649	63,661	34,346	53,209	55,615
% Singletons	39%	39%	36%	29%	40%	31%	35%	35%
Total	**146,548**	**181,188**	**116,915**	**81,693**	**160,200**	**110,905**	**153,555**	**157,204**
	Total number of sequences							
Non-singletons	1,801,130	2,167,248	1,170,904	1,336,753	1,604,740	1,154,977	2,083,712	1,960,304
Singletons	57,609	71,568	41,569	23,649	63,661	34,346	53,209	55,615
% Singletons	3%	3%	3%	2%	4%	3%	2%	3%
Total	**1,858,739**	**2,238,816**	**1,212,473**	**1,360,402**	**1,668,401**	**1,189,323**	**2,136,921**	**2,015,919**

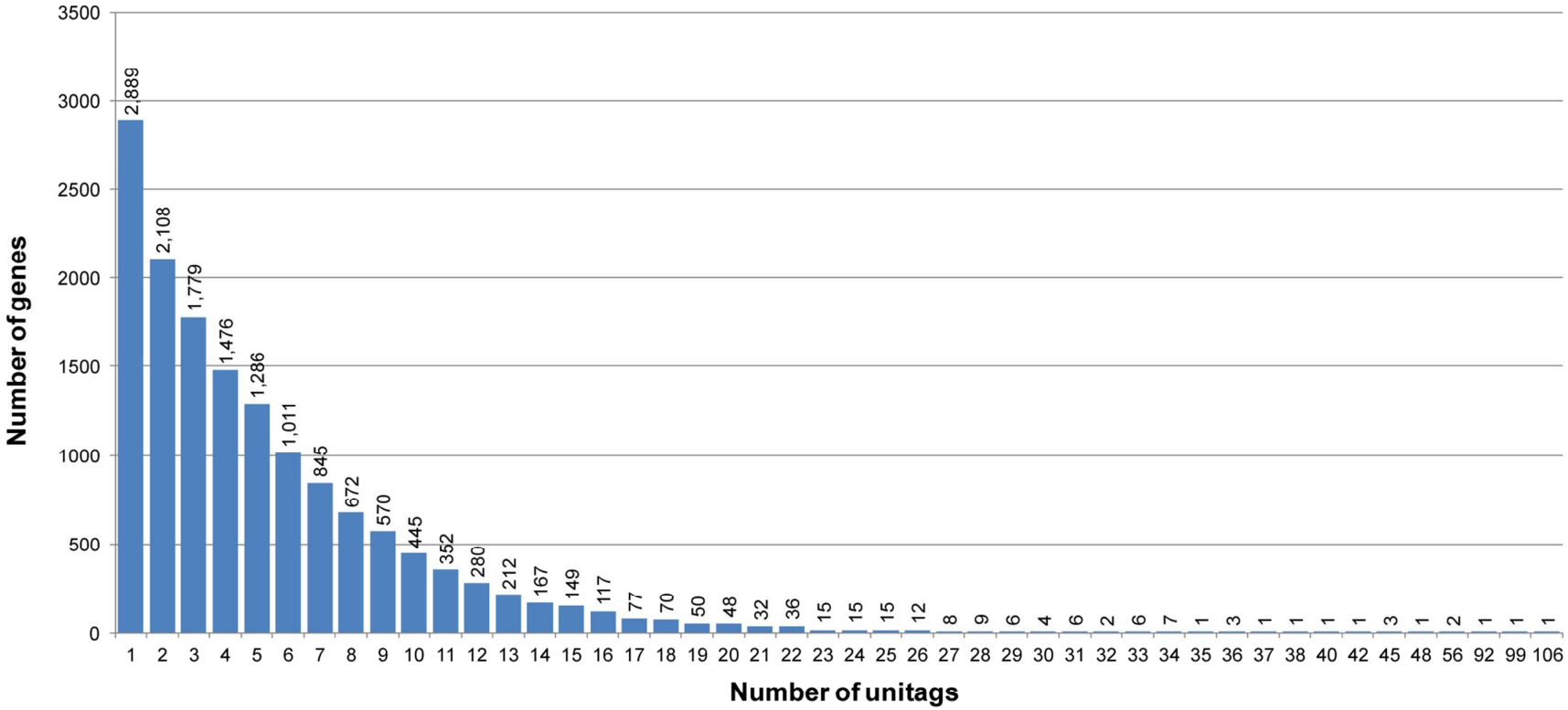

Figure S2 – Mapping of sequences to genes. The number of genes represented by multiple sequence tags (number of tags per gene are indicated on the x-axis and the number of genes are indicated in the y-axis).

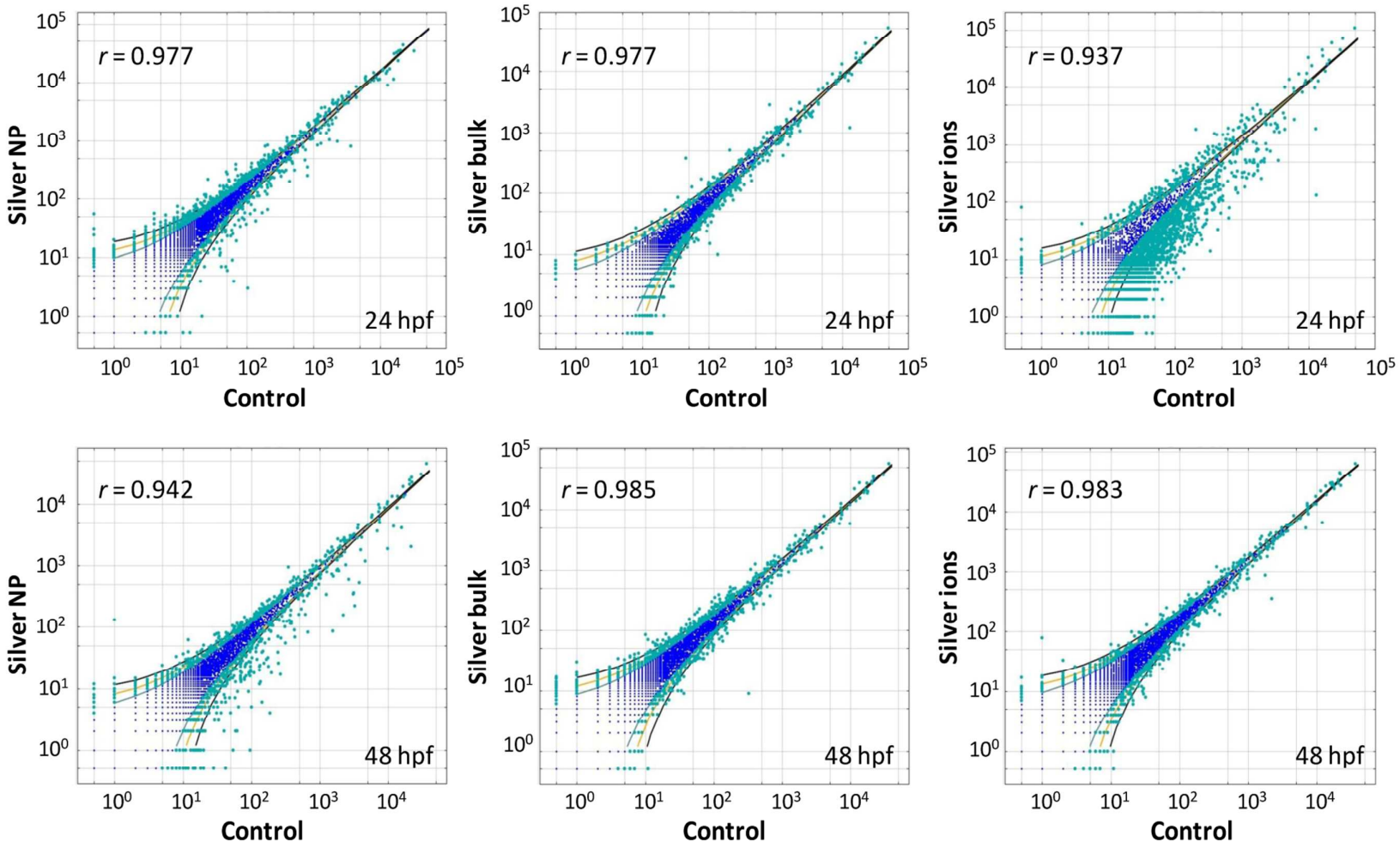

Figure S3 – Gene expression correlation between the different silver treatment libraries and the time-matched control libraries. Coloured dots indicate individual genes (total normalized counts for each gene; values of zero have been replaced with 0.5) and lines indicate confidence intervals (black line – 99.9%, orange line – 99% and blue line – 95%). Genes outside of these confidence intervals (light blue dots) are considered statistically different from the controls. Pearson correlation coefficients are shown in the upper left corner of each plot.

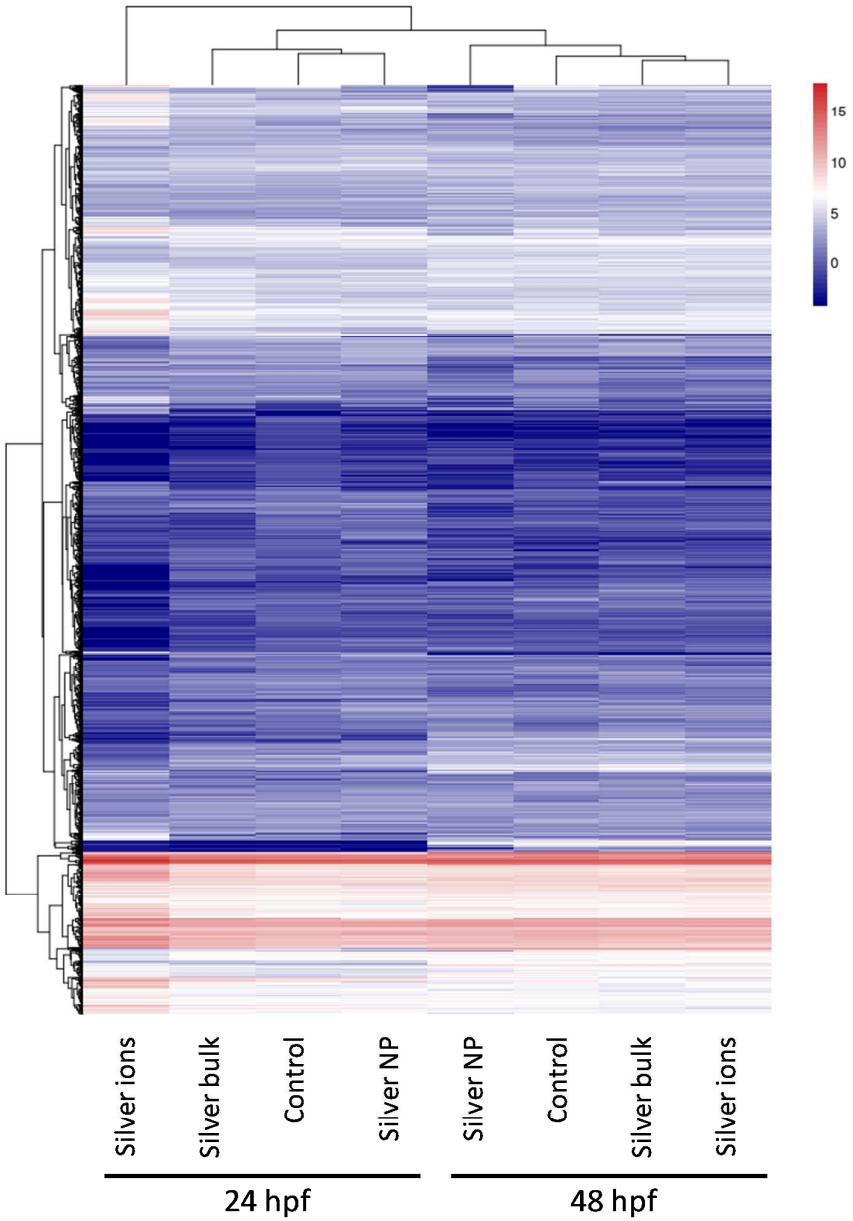

Figure S4 - Heatmap showing differential gene expression across the various silver treatment libraries. This heatmap was created using all differentially expressed genes (adjusted P values < 0.05) using the pheatmap package in R/Bioconductor [16, 17]. The level of gene expression is visualized by using a colour gradient from dark blue (low expression) to dark red (high expression). The following code was used to generate the image: `pheatmap(list_of_DEgenes, color = colorRampPalette(c("navy", "white", "firebrick3"))(50))`.

Biological Processes	24h post-fertilisation			48h post-fertilisation		
	Silver NP	Silver bulk	Silver ions	Silver NP	Silver bulk	Silver ions
translation	70	62	117	60	55	44
translational elongation	8	9	9	5	6	4
regulation of cell cycle	11	7	18	9	7	8
generation of precursor metabolites and energy	13	-	54	21	17	14
ATP metabolic process	-	-	28	9	7	9
cellular respiration	-	-	20	9	6	4
nucleoside triphosphate metabolic process	-	-	29	9	7	9
oxidative phosphorylation	-	-	29	10	6	8
purine nucleoside triphosphate metabolic process	-	-	29	9	7	9
purine nucleotide biosynthetic process	-	-	32	10	8	11
purine nucleotide metabolic process	-	-	34	11	9	12
purine ribonucleoside triphosphate metabolic process	-	-	29	9	7	9
purine ribonucleotide biosynthetic process	-	-	30	10	8	10
purine ribonucleotide metabolic process	-	-	31	11	9	11
ribonucleoside triphosphate metabolic process	-	-	29	9	7	9
ribonucleotide biosynthetic process	-	-	30	10	8	11
ribonucleotide metabolic process	-	-	31	11	9	12
aerobic respiration	-	-	9	5	5	-
energy derivation by oxidation of organic compounds	-	-	20	9	6	-
ATP biosynthetic process	-	-	27	8	-	8
ATP synthesis coupled proton transport	-	-	20	7	-	7
energy coupled proton transport, down electrochemical gradient	-	-	20	7	-	7
hydrogen transport	-	-	22	7	-	7
ion transmembrane transport	-	-	20	7	-	7
nucleoside triphosphate biosynthetic process	-	-	28	8	-	8
proton transport	-	-	22	7	-	7
purine nucleoside triphosphate biosynthetic process	-	-	28	8	-	8
ribonucleoside triphosphate biosynthetic process	-	-	28	8	-	8
nitrogen compound biosynthetic process	-	-	54	-	15	14
cellular di-, tri-valent inorganic cation homeostasis	5	5	-	-	-	-
di-, tri-valent inorganic cation homeostasis	5	5	-	-	-	-
purine ribonucleoside triphosphate biosynthetic process	-	-	28	8	-	8
camera-type eye development	-	-	31	11	-	-
electron transport chain	-	-	16	8	-	-
respiratory electron transport chain	-	-	11	4	-	-
nucleotide biosynthetic process	-	-	-	11	-	12
cation homeostasis	-	6	-	-	-	-
cellular cation homeostasis	-	6	-	-	-	-
cellular chemical homeostasis	-	6	-	-	-	-
cellular ion homeostasis	-	6	-	-	-	-
ATP synthesis coupled electron transport	-	-	9	-	-	-
cell cycle	-	-	49	-	-	-
cellular macromolecule catabolic process	-	-	59	-	-	-
cellular protein catabolic process	-	-	51	-	-	-
chromosome organization	-	-	47	-	-	-
DNA replication	-	-	25	-	-	-
M phase of mitotic cell cycle	-	-	19	-	-	-
macromolecular complex assembly	-	-	40	-	-	-
macromolecule catabolic process	-	-	62	-	-	-
mitotic cell cycle	-	-	24	-	-	-
mRNA metabolic process	-	-	33	-	-	-
mRNA processing	-	-	30	-	-	-
nuclear division	-	-	19	-	-	-
protein catabolic process	-	-	54	-	-	-
protein folding	-	-	35	-	-	-
proteolysis involved in cellular protein catabolic process	-	-	51	-	-	-
response to cadmium ion	-	-	7	-	-	-
response to methylmercury	-	-	7	-	-	-
retina development in camera-type eye	-	-	-	8	-	-
amine biosynthetic process	-	-	-	-	6	-
cellular amino acid biosynthetic process	-	-	-	-	5	-
glycolysis	-	-	-	-	6	-
nucleobase, nucleoside and nucleotide biosynthetic process	-	-	-	-	-	12
nucleobase, nucleoside, nucleotide and nucleic acid biosynthetic process	-	-	-	-	-	12

Figure S5 – Gene Ontology (GO) terms over-represented in differentially expressed gene lists following exposure of zebrafish embryos to silver. DAVID was used to identify over-representation of GO terms for Biological Processes, Cellular Components and Molecular Functions for lists of genes differentially expressed between each treatment and its control (adjusted P values < 0.05), after 24 and 48h of exposure, using the list of all expressed genes as a background. Different shades of blue represent different statistical thresholds for over-representation: dark blue indicates $P < 0.05$ with Benjamini-Hochberg multiple test correction [18], medium and light blue indicate $P < 0.01$ and $P < 0.05$, respectively (without multiple-testing correction). For visualization purposes, only GO terms over-represented with $P < 0.01$ in at least one treatment were included. The numbers in each box indicate the total numbers of genes for each GO term among the list of differentially expressed genes for each treatment. The full dataset for GO analysis over-representation is presented in File S5.

Cellular Components	24h post-fertilisation			48h post-fertilisation		
	Silver NP	Silver bulk	Silver ions	Silver NP	Silver bulk	Silver ions
intracellular non-membrane-bounded organelle	87	63	205	73	73	56
non-membrane-bounded organelle	87	63	205	73	73	56
ribonucleoprotein complex	71	57	129	57	58	48
ribosomal subunit	9	10	15	8	9	9
ribosome	65	52	92	53	53	44
small ribosomal subunit	7	6	7	5	5	5
proteasome complex	8	-	21	10	7	6
proteasome core complex	7	-	10	7	5	-
large ribosomal subunit	-	4	8	-	4	4
proton-transporting ATP synthase complex	-	-	12	6	5	5
respiratory chain	-	4	11	5	-	-
proton-transporting two-sector ATPase complex	-	-	21	7	-	7
cytosol	-	-	-	17	10	10
eukaryotic translation elongation factor 1 complex	4	4	-	-	-	-
mitochondrial inner membrane	-	-	31	13	-	-
mitochondrion	-	-	66	23	-	-
organelle inner membrane	-	-	32	13	-	-
mitochondrial membrane	-	-	36	14	-	-
mitochondrial part	-	-	49	15	-	-
chromosome	-	-	39	-	-	-
envelope	-	-	54	-	-	-
organelle envelope	-	-	54	-	-	-
proton-transporting ATP synthase complex, coupling factor F(o)	-	-	9	-	-	-

Molecular Function	24h post-fertilisation			48h post-fertilisation		
	Silver NP	Silver bulk	Silver ions	Silver NP	Silver bulk	Silver ions
structural constituent of ribosome	62	49	84	49	50	43
structural molecule activity	73	54	123	60	62	53
hydrogen ion transmembrane transporter activity	8	6	31	13	8	9
rRNA binding	6	4	8	4	6	5
monovalent inorganic cation transmembrane transporter activity	-	7	33	14	8	9
inorganic cation transmembrane transporter activity	-	8	41	14	9	10
threonine-type endopeptidase activity	7	-	10	7	5	-
threonine-type peptidase activity	7	-	10	7	5	-
translation elongation factor activity	6	7	11	-	-	-
translation factor activity, nucleic acid binding	9	12	33	-	-	-
RNA binding	22	-	84	-	-	-
cytochrome-c oxidase activity	-	-	10	5	-	-
heme-copper terminal oxidase activity	-	-	10	5	-	-
oxidoreductase activity, acting on heme group of donors	-	-	10	5	-	-
oxidoreductase activity, acting on heme group of donors, oxygen as acceptor	-	-	10	5	-	-
translation initiation factor activity	-	-	23	-	-	-
NADH dehydrogenase (quinone) activity	-	-	10	-	-	-
NADH dehydrogenase (ubiquinone) activity	-	-	10	-	-	-
NADH dehydrogenase activity	-	-	10	-	-	-
oxidoreductase activity, acting on NADH or NADPH, quinone or similar compound as acceptor	-	-	10	-	-	-

Figure S5 (continued)

Table S2 – List of genes differentially expressed in a treatment-specific manner.

		Expression values (normalized counts per million)		Fold change (+direction)				Adjusted P values			
Treatment	**Ensembl Gene ID**	**24hpf**	**48hpf**	**24hpf**		**48hpf**		**24hpf**	**48hpf**	**Gene symbol**	**Gene Description**
Silver bulk	ENSDARG00000069763	239	189	1.4	DOWN	1.5	DOWN	1.9E-02	6.5E-04	*etv5a*	ETS translocation variant 5 [Source:RefSeq peptide;Acc:NP_001119933]
Silver ions	ENSDARG00000075016	53.3	17.8	2	UP	2.4	DOWN	9.8E-03	4.2E-02	*A5WUQ7_DANRE*	Novel protein similar to vertebrate apolipoprotein B (Including Ag(X) antigen) (APOB) Fragment [Source:UniProtKB/TrEMBL;Acc:A5WUQ7]
Silver ions	ENSDARG00000012399	279	204	1.6	UP	1.5	UP	1.1E-06	1.1E-02	*adssl*	adenylosuccinate synthase, like [Source:RefSeq peptide;Acc:NP_775344]
Silver ions	ENSDARG00000007413	42.6	22.4	5.5	DOWN	2.4	DOWN	6.2E-05	1.4E-02	*arid2*	AT-rich interactive domain-containing protein 2 [Source:RefSeq peptide;Acc:NP_001071231]
Silver ions	ENSDARG00000039515	189	99.6	2.3	DOWN	2	DOWN	1.8E-09	1.0E-06	*atf4b1*	Cyclic AMP-dependent transcription factor ATF-4 (cAMP-dependent transcription factor ATF-4)(Activating transcription factor 4) [Source:UniProtKB/Swiss-Prot;Acc:Q6NW59]
Silver ions	ENSDARG00000014313	149	181	2.5	DOWN	1.5	DOWN	6.1E-08	7.2E-04	*atp5j*	ATP synthase-coupling factor 6, mitochondrial [Source:RefSeq peptide;Acc:NP_998472]
Silver ions	ENSDARG00000045543	297	382	1.9	UP	1.3	UP	1.8E-14	1.9E-02	*atp6v1f*	V-type proton ATPase subunit F [Source:RefSeq peptide;Acc:NP_001002526]
Silver ions	ENSDARG00000034961	154	100	3.1	DOWN	2.3	DOWN	4.5E-11	2.6E-11	*bzw1b*	Basic leucine zipper and W2 domain-containing protein 1-B [Source:UniProtKB/Swiss-Prot;Acc:Q803N9]
Silver ions	ENSDARG00000057013	41.1	117	3.3	DOWN	1.7	DOWN	1.5E-05	3.7E-04	*cadm3*	cell adhesion molecule 3 [Source:RefSeq peptide;Acc:NP_001038711]
Silver ions	ENSDARG00000069093	94.4	163	3.3	DOWN	1.5	DOWN	2.1E-09	8.3E-03	*col2a1a*	collagen alpha-1(II) chain [Source:RefSeq peptide;Acc:NP_571367]
Silver ions	ENSDARG00000018002	82.2	161	2	DOWN	1.7	UP	3.4E-04	3.5E-03	*dci*	Dci protein Fragment [Source:UniProtKB/TrEMBL;Acc:Q6DBW7]
Silver ions	ENSDARG00000012066	79.2	244	4	DOWN	1.4	UP	1.8E-07	2.9E-02	*Dcn*	decorin [Source:RefSeq peptide;Acc:NP_571772]

Silver ions	ENSDARG00000020913	24.4	5.41	3.6	DOWN	4.6	DOWN	4.6E-03	1.0E-02	*ddx56*	probable ATP-dependent RNA helicase DDX56 [Source:RefSeq peptide;Acc:NP_001003876]
Silver ions	ENSDARG00000032653	3.05	20.1	17.9	DOWN	5.7	UP	9.1E-04	3.4E-02	*fam60a*	family with sequence similarity 60, member A [Source:RefSeq peptide;Acc:NP_001020702]
Silver ions	ENSDARG00000062997	24.4	9.27	8.1	DOWN	3.2	DOWN	5.7E-04	3.0E-02	*hyal2*	Novel protein similar to vertebrate hyaluronoglucosaminidase 2 (HYAL2) Fragment [Source:UniProtKB/TrEMBL;Acc:Q1LXC3]
Silver ions	ENSDARG00000041516	111	29.3	1.6	UP	2.4	DOWN	1.3E-03	1.9E-03	*LOC100331938*	-
Silver ions	ENSDARG00000058337	137	63.3	2.2	DOWN	1.7	DOWN	4.9E-07	3.5E-02	*nop58*	NOP58 ribonucleoprotein homolog [Source:RefSeq peptide;Acc:NP_001009889]
Silver ions	ENSDARG00000020143	7.61	36.3	12.8	DOWN	2.8	UP	1.2E-02	4.2E-02	*pah*	phenylalanine-4-hydroxylase [Source:RefSeq peptide;Acc:NP_956845]
Silver ions	ENSDARG00000030638	32	93.5	2.7	DOWN	2.4	DOWN	5.4E-03	3.2E-12	*pdlim7*	Pdlim7 protein [Source:UniProtKB/TrEMBL;Acc:Q6NWL9]
Silver ions	ENSDARG00000035146	95.9	66.4	1.7	DOWN	1.9	DOWN	1.6E-02	1.4E-03	*polr2j*	polymerase (RNA) II (DNA directed) polypeptide J [Source:RefSeq peptide;Acc:NP_001019571]
Silver ions	ENSDARG00000015474	22.8	27.8	2.6	DOWN	2.1	DOWN	1.6E-02	2.7E-02	*ppp2r5ea*	protein phosphatase 2, regulatory subunit B', epsilon isoform a [Source:RefSeq peptide;Acc:NP_919396]
Silver ions	ENSDARG00000027088	57.9	91.1	3.2	DOWN	1.6	DOWN	1.8E-05	2.3E-02	*ptgds*	prostaglandin D2 synthase, brain [Source:RefSeq peptide;Acc:NP_998799]
Silver ions	ENSDARG00000052617	350	221	2.3	DOWN	1.5	DOWN	0.0E+00	1.9E-04	*raver1*	ribonucleoprotein, PTB-binding 1 [Source:RefSeq peptide;Acc:NP_001018503]
Silver ions	ENSDARG00000016088	42.6	37.1	1.8	UP	1.9	DOWN	3.5E-02	2.8E-02	*rtn2a*	reticulon 2a [Source:RefSeq peptide;Acc:NP_001025136]
Silver ions	ENSDARG00000013721	73.1	35.5	1.9	DOWN	2	DOWN	4.6E-03	2.2E-02	*si:ch211-215l11.5*	im:6895556 [Source:RefSeq peptide;Acc:NP_001157278]
Silver ions	ENSDARG00000019231	28.9	49.4	3.5	DOWN	2.3	UP	1.7E-03	3.8E-02	*spna2*	spectrin alpha chain, brain [Source:RefSeq peptide;Acc:NP_001091958]
Silver ions	ENSDARG00000052712	1390	1420	2.1	UP	1.1	DOWN	2.4E-90	1.0E-02	*suclg1*	succinyl-CoA ligase [Source:RefSeq peptide;Acc:NP_001002577]
Silver ions	ENSDARG00000040031	393	342	3.4	DOWN	1.3	DOWN	0.0E+00	1.1E-02	*tardbp*	TAR DNA-binding protein 43 [Source:RefSeq peptide;Acc:NP_958884]
Silver ions	ENSDARG00000031164	62.4	191	1.5	UP	2.5	UP	3.0E-02	2.9E-10	*tuba8l2*	tubulin alpha-4A chain [Source:RefSeq peptide;Acc:NP_956985]
Silver ions	ENSDARG00000078075	45.7	30.9	2.4	DOWN	2.1	DOWN	7.7E-03	2.5E-02	*zgc:101577*	Uncharacterized protein C6orf106 homolog

											[Source:UniProtKB/Swiss-Prot;Acc:Q5BL31]
Silver ions	ENSDARG00000036834	888	71.8	2.1	DOWN	1.8	DOWN	0.0E+00	2.0E-03	*zgc:109868*	cytokeratin-like [Source:RefSeq peptide;Acc:NP_001017824]
Silver ions	ENSDARG00000037405	28.9	6.18	2	UP	3.8	DOWN	7.5E-03	3.4E-02	*zgc:112083*	MBD2 (methyl-CpG-binding protein)-interacting zinc finger protein [Source:RefSeq peptide;Acc:NP_001017764]
Silver ions	ENSDARG00000038076	580	541	1.2	UP	1.2	DOWN	3.8E-02	3.4E-02	*zgc:73345*	Reactive oxygen species modulator 1 (ROS modulator 1)(Protein MGR2 homolog) [Source:UniProtKB/Swiss-Prot;Acc:Q6NYD1]
Silver NP	ENSDARG00000077653	0	0	0	DOWN	0	DOWN	1.0E-03	2.9E-04	-	-
Silver NP	ENSDARG00000019547	204	31.2	2	DOWN	6.7	DOWN	0.0E+00	0.0E+00	*aaas*	aladin [Source:RefSeq peptide;Acc:NP_998390]
Silver NP	ENSDARG00000020761	175	90.9	2.6	UP	2.3	UP	2.3E-09	2.1E-03	*arrdc2*	arrestin domain-containing protein 2 [Source:RefSeq peptide;Acc:NP_956233]
Silver NP	ENSDARG00000056258	20.5	1.36	3.6	DOWN	24.3	DOWN	9.9E-07	3.1E-05	*cdc27*	cell division cycle protein 27 homolog [Source:RefSeq peptide;Acc:NP_958857]
Silver NP	ENSDARG00000045768	8.21	19	6.3	DOWN	4.3	DOWN	2.8E-07	1.1E-06	*cry1a*	cryptochrome 1a isoform 2 [Source:RefSeq peptide;Acc:NP_571864]
Silver NP	ENSDARG00000035603	5.75	1.36	5.1	DOWN	13	DOWN	1.2E-03	3.0E-02	*dao.2*	D-amino acid oxidase [Source:RefSeq peptide;Acc:NP_999897]
Silver NP	ENSDARG00000027813	285	335	1.4	UP	1.4	UP	1.1E-02	8.9E-03	*nus1*	Nogo-B receptor Precursor (NgBR)(Nuclear undecaprenyl pyrophosphate synthase 1 homolog) [Source:UniProtKB/Swiss-Prot;Acc:Q6DHR8]
Silver NP	ENSDARG00000009640	1550	2180	1.2	DOWN	1.3	UP	2.7E-06	1.4E-12	*psmb1*	proteasome subunit beta type-1 [Source:RefSeq peptide;Acc:NP_001003889]
Silver NP	ENSDARG00000017886	131	155	2	UP	1.9	UP	4.8E-04	1.1E-03	*si:dkeyp-116g9.2*	Zinc finger protein ZNF-U69274 [Source:UniProtKB/TrEMBL;Acc:Q6TNP6]
Silver NP	ENSDARG00000037965	326	274	1.7	UP	1.7	UP	1.2E-06	2.8E-04	*srrm2*	Srrm2 protein [Source:UniProtKB/TrEMBL;Acc:Q503X8]
Silver NP	ENSDARG00000090442	237	129	3.6	UP	1.7	UP	4.7E-20	4.9E-02	*wu:fc54d09*	-
Silver NP	ENSDARG00000016830	208	236	1.7	UP	1.5	UP	1.5E-04	3.6E-02	*zgc:92164*	Ribosomal protein S6 modification-like protein B [Source:UniProtKB/Swiss-Prot;Acc:Q66HZ2]
Silver NP	ENSDARG00000008218	92	115	2	DOWN	2	DOWN	2.6E-06	8.6E-06	*znf410*	zinc finger protein 410 [Source:RefSeq peptide;Acc:NP_991216]

REFERENCES

1. Scown, T. M.; Santos, E. M.; Johnston, B. D.; Gaiser, B.; Baalousha, M.; Mitov, S.; Lead, J. R.; Stone, V.; Fernandes, T. F.; Jepson, M.; van Aerle, R.; Tyler, C. R., Effects of aqueous exposure to silver nanoparticles of different sizes in rainbow trout. *Toxicol Sci* **2010,** *115*, (2), 521-34.
2. Boutilier, R.; Heming, T.; Iwama, G., Appendix: Physicochemical Parameters for use in Fish Respiratory Physiology. *Fish Physiology* **1984,** *10*, (A), 403–430.
3. Matsumura, H.; Yoshida, K.; Luo, S.; Kimura, E.; Fujibe, T.; Albertyn, Z.; Barrero, R. A.; Kruger, D. H.; Kahl, G.; Schroth, G. P.; Terauchi, R., High-throughput SuperSAGE for digital gene expression analysis of multiple samples using next generation sequencing. *PLoS One* **2010,** *5*, (8), e12010.
4. Pinto, P. I.; Matsumura, H.; Thorne, M. A.; Power, D. M.; Terauchi, R.; Reinhardt, R.; Canario, A. V., Gill transcriptome response to changes in environmental calcium in the green spotted puffer fish. *BMC Genomics 11*, 476.
5. Gilardoni, P. A.; Schuck, S.; Jungling, R.; Rotter, B.; Baldwin, I. T.; Bonaventure, G., SuperSAGE analysis of the Nicotiana attenuata transcriptome after fatty acid-amino acid elicitation (FAC): identification of early mediators of insect responses. *BMC Plant Biol 10*, 66.
6. Molina, C.; Rotter, B.; Horres, R.; Udupa, S. M.; Besser, B.; Bellarmino, L.; Baum, M.; Matsumura, H.; Terauchi, R.; Kahl, G.; Winter, P., SuperSAGE: the drought stress-responsive transcriptome of chickpea roots. *BMC Genomics* **2008,** *9*, 553.
7. Matsumura, H.; Reich, S.; Ito, A.; Saitoh, H.; Kamoun, S.; Winter, P.; Kahl, G.; Reuter, M.; Kruger, D. H.; Terauchi, R., Gene expression analysis of plant host-pathogen interactions by SuperSAGE. *Proc Natl Acad Sci U S A* **2003,** *100*, (26), 15718-23.
8. Vesterlund, L.; Jiao, H.; Unneberg, P.; Hovatta, O.; Kere, J., The zebrafish transcriptome during early development. *BMC Dev Biol* **2011,** *11*, (1), 30.
9. Yamaguchi, H.; Fukuoka, H.; Arao, T.; Ohyama, A.; Nunome, T.; Miyatake, K.; Negoro, S., Gene expression analysis in cadmium-stressed roots of a low cadmium-accumulating solanaceous plant, Solanum torvum. *J Exp Bot 61*, (2), 423-37.
10. Poole, R. L.; Barker, G. L.; Werner, K.; Biggi, G. F.; Coghill, J.; Gibbings, J. G.; Berry, S.; Dunwell, J. M.; Edwards, K. J., Analysis of wheat SAGE tags reveals evidence for widespread antisense transcription. *BMC Genomics* **2008,** *9*, 475.
11. t Hoen, P. A. C.; Ariyurek, Y.; Thygesen, H. H.; Vreugdenhil, E.; Vossen, R. H. A. M.; de Menezes, R. X.; Boer, J. M.; van Ommen, G. J. B.; den Dunnen, J. T., Deep sequencing-based expression analysis shows major advances in robustness, resolution and inter-lab portability over five microarray platforms. *Nucleic Acids Research* **2008,** *36*, (21).
12. Hegedus, Z.; Zakrzewska, A.; Agoston, V. C.; Ordas, A.; Racz, P.; Mink, M.; Spaink, H. P.; Meijer, A. H., Deep sequencing of the zebrafish transcriptome response to mycobacterium infection. *Molecular immunology* **2009,** *46*, (15), 2918-30.
13. Wang, E. T.; Sandberg, R.; Luo, S.; Khrebtukova, I.; Zhang, L.; Mayr, C.; Kingsmore, S. F.; Schroth, G. P.; Burge, C. B., Alternative isoform regulation in human tissue transcriptomes. *Nature* **2008,** *456*, (7221), 470-6.
14. Pan, Q.; Shai, O.; Lee, L. J.; Frey, B. J.; Blencowe, B. J., Deep surveying of alternative splicing complexity in the human transcriptome by high-throughput sequencing. *Nature genetics* **2008,** *40*, (12), 1413-5.
15. Kimmel, C. B.; Ballard, W. W.; Kimmel, S. R.; Ullmann, B.; Schilling, T. F., Stages of embryonic development of the zebrafish. *Dev Dyn* **1995,** *203*, (3), 253-310.
16. R Development Core Team. R: A language and environment for statistical computing. *R Foundation for Statistical Computing, Vienna, Austria.* **2012,** *ISBN 3-900051-07-0*, (http://www.R-project.org/).

17. Kolde, R., pheatmap: Pretty Heatmaps. R package version 0.7.3. (http://CRAN.R-project.org/package=pheatmap). **2012**.
18. Benjamini, Y.; Hochberg, Y., Controlling the false discovery rate: a practical and powerful approach to multiple testing. *Journal of the Royal Statistical Society B (Methodological)* **1995,** *57*, (1), 289-300.